Available online at www.sciencedirect.com

SciVerse ScienceDirect

Ceramics International 38 (2012) 6145–6149

CERAMICS INTERNATIONAL

www.elsevier.com/locate/ceramint

Aqueous sol–gel synthesis of zirconium titanate ($ZrTiO_4$) nanoparticles using chloride precursors

E. Salahinejad[a,b,c], M.J. Hadianfard[c], D.D. Macdonald[b,d], I. Karimi[c], D. Vashaee[e], L. Tayebi[a,f,*]

[a]*Helmerich Advanced Technology Research Center, School of Materials Science and Engineering, Oklahoma State University, OK 74106, USA*
[b]*Center for Electrochemical Science and Technology, Department of Materials Science and Engineering, Pennsylvania State University, University Park, PA 16802, USA*
[c]*Department of Materials Science and Engineering, School of Engineering, Shiraz University, Zand Blvd., 7134851154, Shiraz, Iran*
[d]*Center for Research Excellence in Corrosion, King Fahd University of Petroleum and Minerals, Dhahran 31261, Saudi Arabia*
[e]*Helmerich Advanced Technology Research Center, School of Electrical and Computer Engineering, Oklahoma State University, OK 74106, USA*
[f]*School of Chemical Engineering, Oklahoma State University, Stillwater, OK 74078, USA*

Received 7 April 2012; received in revised form 22 April 2012; accepted 26 April 2012
Available online 3 May 2012

Abstract

Zirconium titanate powders were synthesized by a straightforward sol–gel method using zirconium and titanium chlorides as metal precursors, deionized water as solvent and oxygen donor, and a NaOH solution for adjusting pH to 7. According to transmission electron microscopy, amorphous particles of nearly 5 nm in size with a relatively spherical morphology were prepared. Thermogravimetry and differential scanning calorimetery analyses on the xerogel at a heating rate of 10 °C/min indicated a crystallization temperature of 690 °C, which is comparable with previous reports. Furthermore, via differential scanning calorimetery studies using the Kissinger's equation, the activation energy for $ZrTiO_4$ crystallization was determined to be 850 kJ/mol. Structural evaluations in the isothermal regime, using X-ray diffraction experiments, implied the onset of $ZrTiO_4$ crystallization at 550 °C.

Keywords: A. Sol–gel processes; B. X-ray methods; C. Thermal properties

1. Introduction

Zirconium titanate ($ZrTiO_4$) is an attractive ceramic for electronic, optical, chemical, catalytic, and biomedical applications [1–6], but demanding high purity and homogeneity. One of the promising approaches to synthesize homogeneous ceramic powders is the sol–gel process. In this method, when a high level of homogeneity is achieved, the obtained amorphous materials crystallize at temperatures of several hundred degrees lower than in classical routes, such as traditional melting and powder processing [7–11]. In addition, as a result of the development of high specific surface area powders by the sol–gel process, much lower sintering temperatures are required.

The sol–gel preparation of zirconium titanate can be conducted by hydrolysis and condensation of inorganic salts [9,12,13] or alkoxides [14–16] as precursors, where the control of the hydrolysis and condensation processes is essential when establishing procedures especially for the latter. A number of non-hydrolytic sol–gel processes have been also focused on producing zirconium titanate powders [10,11]. On the other hand, nanostructured TiO_2–ZrO_2 powders and thin films have been prepared by an aqueous particulate sol–gel route from titanium isopropoxide and zirconium acetate hydrate as precursors [17]. However, to our knowledge, no work has been reported to date on the aqueous particulate sol–gel synthesis of zirconium titanate from chloride precursors.

In this research, a straightforward aqueous particulate sol–gel method, as an environmentally friendly processing, was used to produce zirconium titanate powders. The process

*Corresponding author. Tel.: +1 918 594 8634.
E-mail address: lobat.tayebi@okstate.edu (L. Tayebi).

0272-8842/$36.00
http://dx.doi.org/10.1016/j.ceramint.2012.04.064

is based on the hydrolysis of metal chlorides, in which alkoxide functions are formed in situ. One of the advantages of this route is employing an alternative (chloride precursors) to alkoxide precursors used in polymeric sol–gel methods to develop a product at lower cost, which is a significant attribute. This paper focuses on the sol–gel synthesis and characterization of zirconium titanate starting from $ZrCl_4$ and $TiCl_4$ as the metal precursors.

2. Materials and methods

2.1. Sample preparation

18.2 mmol of zirconium tetrachloride ($ZrCl_4$, Alfa Aesar, 99.5%) was gradually added to 400 mL of deionized water and stirred for 15 min. 18.2 mmol of titanium tetrachloride ($TiCl_4$, Alfa Aesar, 99.99%) was added dropwise to the solution and magnetically stirred for 2 h, leading to a solution of pH 0.98 measured using a calibrated pH meter (Sartorius Professional Meter PP-15). Subsequently, an aqueous solution of NaOH (2 M) was added dropwise under magnetic stirring conditions until the pH value approached 7, forming a white hydrogel. After aging for 30 min, in order to remove chloride ion, the hydrogel was rinsed several times with deionized water, and the absence of chloride ions was checked using $AgNO_3$. The obtained sample was centrifuged at 6000 rpm for 10 min, washed with ethanol, again centrifuged, and finally dried at 60 °C for 2 h, developing white agglomerated powders (xerogel). The obtained powder was calcined at 500, 550, and 600 °C for 1 h with a heating rate of 10 °C/min in a nitrogen atmosphere.

2.2. Structural and thermal characterization

A transmission electron microscope (TEM, JEOL JEM-2100) operating at an acceleration voltage of 200 kV was used to evaluate the powder particle size and morphology. To do so, a small amount of the powder was dispersed in ethanol, ultrasonicated for 15 min, and then dropped on a carbon grid. To study the thermal behavior of the xerogel, simultaneous thermo-gravimetry and differential scanning calorimetery analyses (TGA/DSC, Netzsch, STA 449 F1 Jupiter®) were performed under a flowing argon atmosphere in an alumina container. The X-ray diffraction (XRD) pattern of the xerogel and calcined powders was recorded by a Bruker AXS Inco. diffractometer using Cu Kα radiation ($\lambda = 1.54056$ Å).

3. Results and discussion

The TEM observations of the xerogel powder particles (before calcination) show two typical features. As depicted in Fig. 1(a), despite dispersion in ethanol and ultrasonication, some agglomerated particles of 50–100 nm in size can be still seen, making it difficult to distinguish the real particle size and morphology. This strong tendency toward

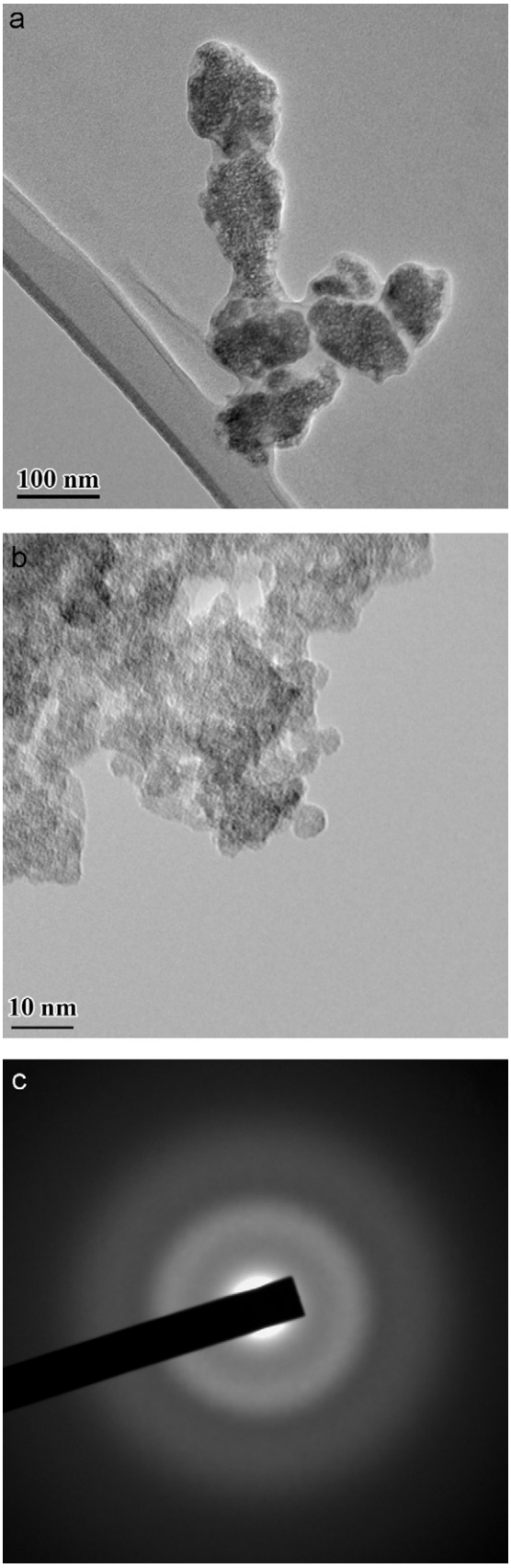

Fig. 1. TEM micrograph of the xerogel powder particles showing agglomeration (a), TEM micrograph of the xerogel powder particles in a higher magnification indicating nanoparticles of 5 nm in size (b), and the related SAD pattern suggesting an amorphous phase (b).

agglomeration is due to the significant surface-to-volume ratio and surface tension of nanoparticles. Nonetheless, according to Fig. 1(b), on the edge of the agglomerated particles, powder particles of approximately 5 nm in diameter with a relatively spherical morphology can be recognized. The related selected area diffraction (SAD) pattern (Fig. 1(c)) indicates homogenous featureless diffraction halos attributed to an amorphous structure. No diffraction spots or sharp rings associated with crystalline phases can be observed, suggesting the synthesis of fully amorphous nanoparticles.

The TGA and DSC profiles of the xerogel at a heating rate of 10 °C/min are provided in Fig. 2. In the TGA curve, a pronounced weight loss of 15% is observed from 100 to 250 °C. A broad endothermic peak at around 120 °C and a sharp exothermic peak at 690 °C are also observed in the DSC curve. Considering both analyses simultaneously, it is evident that the first event, the endothermic one with a considerable weight loss, is due to the removal of residual water and chloride during heating. On the other hand, the second sharp event was accompanied by no weight loss and is attributed to crystallization of the amorphous phase developed by the sol–gel method, as verified by XRD and TEM studies below. In accordance with the DSC profile, the onset crystallization temperature and crystallization peak temperature are 575 and 690 °C, respectively.

To study the kinetic behavior of the crystallization event, further DSC experiments on the xerogel were carried out at different heating rates of 20, 30, 40, and 50 °C/min. Based on the data shown in Fig. 3(a), by increasing the heating rate, the crystallization peak is shifted to higher temperatures since the crystallization process from an amorphous phase is a diffusional and thermally-activated transformation controlled via nucleation and growth. The activation energy for crystallization (E_c) can be determined by the Kissinger's equation [18]:

$$\ln\left(\frac{Tc^2}{C}\right) = \frac{Ec}{RTc} + \text{const.} \quad (1)$$

where T_c, C, and R are the crystallization peak temperature, heating rate, and universal gas constant respectively. Fig. 3(b) demonstrates the linear relationship between $\ln(T_c^2/C)$ and $(1/T_c)$. From the slope of the curve, the value of E_c can be easily determined to be 850 kJ/mol. It has been reported that

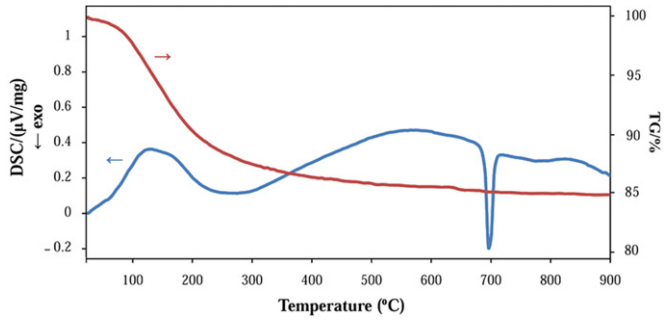

Fig. 2. TGA and DSC profiles of the xerogel at a heating rate of 10 °C/min.

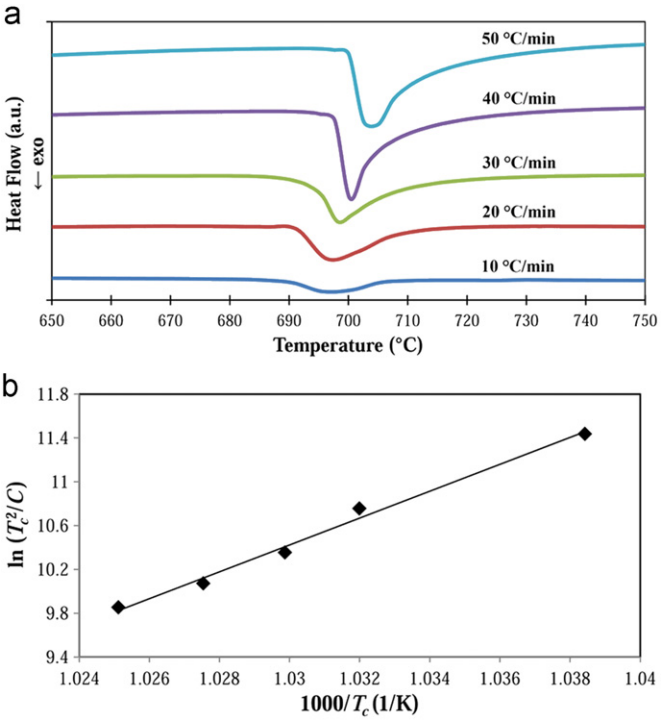

Fig. 3. DSC curves of $ZrTiO_4$ crystallization obtained at the different heating rates (a) and Kissinger plot for $ZrTiO_4$ crystallization (b).

the activation energy of $ZrTiO_4$ crystallization from amorphous powders prepared by sol–gel methods is 620 kJ/mol with the crystallization peak appearing at 642 °C [19] and 139–323 kJ/mol with the peak becoming evident at 530–680 °C [2]. Compared to the results of this work, it can be concluded that the activation energy of $ZrTiO_4$ crystallization strongly depends on the preparation conditions. The activation energy of crystallization calculated by the Kissinger's equation is the activation energy required for growth [20]. The growth of nuclei needs an atomic rearrangement of the constituents, which is closely related to their diffusivity. Indeed, the difference of the activation energy calculated for this material synthesized by different procedures might be due to differences in the particle size, degree of hydration, homogeneity, and short-range order of the amorphous phase [2].

To assess the structural evolution in the course of heating, particularly in the case of isothermal heat treatment, the XRD analyses were conducted on the xerogel before and after calcination at 500, 550, and 600 °C, as represented in Fig. 4. The broad halo pattern of the xerogel [Fig. 4(a)] suggests a typical amorphous pattern, as confirmed by its SAD pattern [Fig. 1(c)]. As can be observed, the amorphous structure is still stable at 500 °C [Fig. 4(b)]; however, the appearance of a number of $ZrTiO_4$ reflections in the XRD pattern of the sample calcined at 550 °C, provided in Fig. 4(c), is indicative of the onset of structural ordering and crystallization. Fig. 4(d) specifies the XRD pattern of the powder calcined at 600 °C, inferring the crystalline $ZrTiO_4$ phase with a crystallite size of 13 nm, determined by the EVA software using the Scherrer equation for the XRD maxima. The instrument broadening

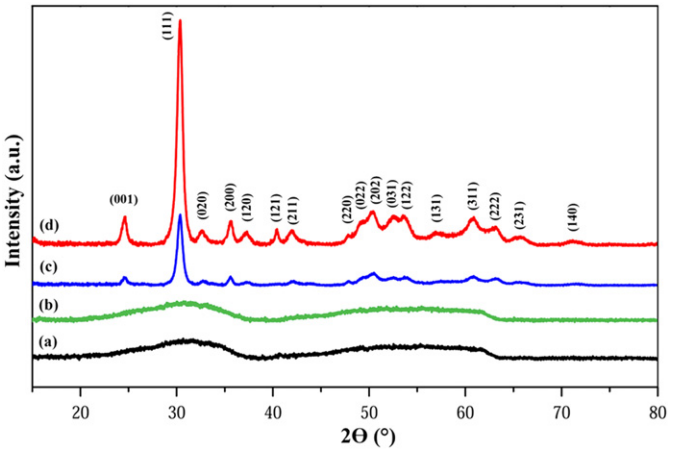

Fig. 4. XRD pattern of the xerogel (a) and the powders calcined at 500 °C (b), 550 °C (c), and 600 °C (d).

was calibrated by using a standard sample. Note that it is reasonable to neglect the strain contribution to broadening at low Bragg angles [21]. The XRD reflections were also confirmed by the ICSD reference code of 00-034-0415 for zirconium titanate with the orthorhombic α-PbO_2 type structure, in which Zr and Ti atoms are in octahedral oxygen coordination. No XRD reflection corresponding to TiO_2 and ZrO_2 can be detected. The direct crystallization of $ZrTiO_4$ at the low temperature is due to the high level of homogeneity of the xerogel. It has been reported that, in the case of low homogeneity, TiO_2 crystallization occurs before crystallization into $ZrTiO_4$ [22]. The TEM micrograph and SAD pattern of the sample calcined at 600 °C are illustrated in Fig. 5. Compared to the xerogel (Fig. 1), the powder particles have grown, with the driving force being a reduction in the surface energy, and have approached an average size of 50 nm with a relatively wide size range of 20–100 nm. Moreover, the high crystallinity of this powder results in distinct Debye–Scherrer diffraction spots in the SAD pattern (Fig. 5(b)).

As shown above, based on the XRD analysis, the crystallization is initiated at 550 °C (even at lower temperatures), but the crystallization peak of the DSC test is located at 690 °C. The difference of the crystallization behavior detected from the DSC and XRD evaluations is due to the difference between the thermal regimes applied. During the DSC analysis, heating is continuous at a rate of 10 °C/min; nonetheless, the XRD patterns were obtained from the samples calcined at the different temperatures for 1 h under isothermal conditions, where time for the diffusional transformation of crystallization is provided, allowing the onset of crystallization at low temperatures.

In conclusion, typical advantages of this processing route described in this paper are: (i) it is a straightforward and uncomplicated procedure, (ii) it allows for the successful synthesis of $ZrTiO_4$ nanoparticles with a crystallization temperature much lower than in classical $ZrTiO_4$ processing methods, and (iii) it is capable of producing low cost powders compared to polymeric sol–gel methods using alkoxide precursors.

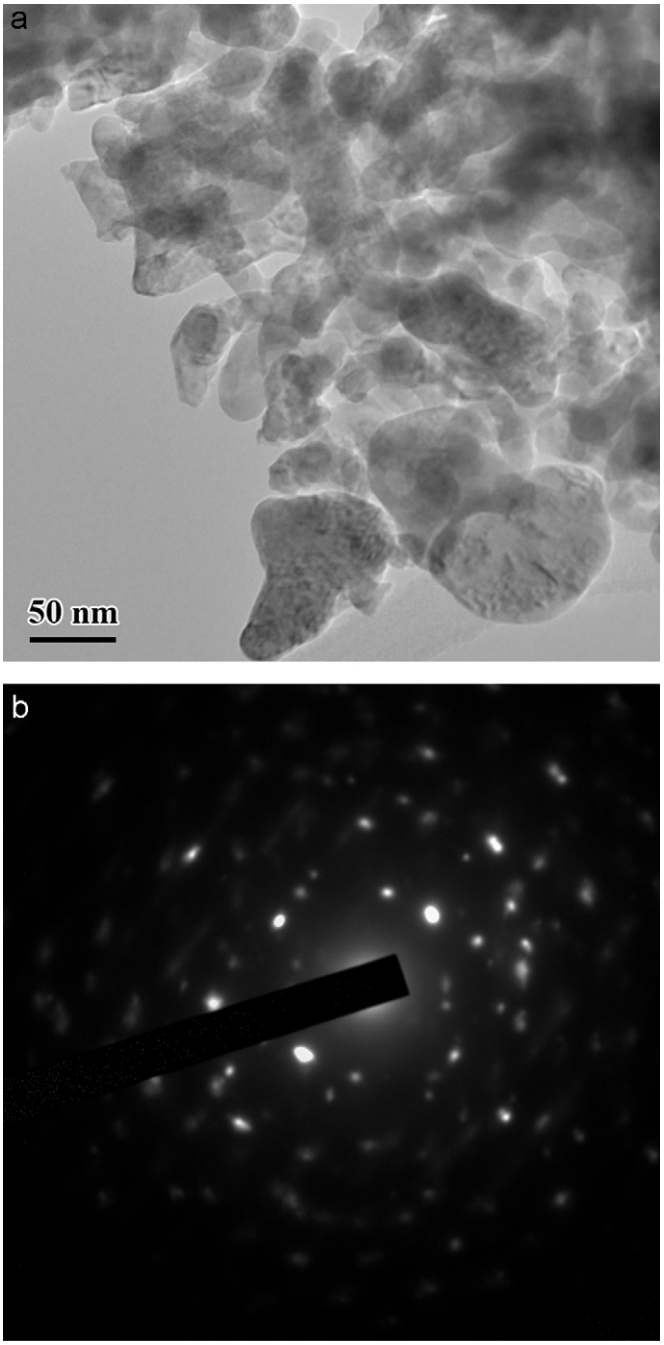

Fig. 5. TEM micrograph (a) and SAD pattern (b) of the powder specimen calcined at 600 °C.

4. Conclusions

In this work, an aqueous sol–gel procedure using zirconium and titanium chlorides was developed to synthesize $ZrTiO_4$ powder. From this study, the following conclusions could be drawn:

- According to the TEM studies, amorphous particles of almost 5 nm in size with a relatively spherical morphology were prepared.

- The crystallization peak temperature of the amorphous powder prepared by the sol–gel route was found to be nearly 690 °C, as determined by the DSC/TGA experiment at a heating rate of 10 °C/min.
- Using the Kissinger's equation, the activation energy for $ZrTiO_4$ crystallization was determined to be 850 kJ/mol.
- Calcination at 550 °C for 1 h developed $ZrTiO_4$ nanocrystals of 15 nm in size determined by XRD. In addition, high crystallinity and particle growth were confirmed by TEM studies.

Acknowledgments

This work was partially supported by AFOSR under Grant no. FA9550-10-1-0010 and the National Science Foundation (NSF) under Grant no. 0933763.

References

[1] L. Pandolfi, S. Kaciulis, G. Padeletti, A. Cusma, M. Viticoli, Deposition and characterization of $ZrTiO_4$ thin films, Surface and Interface Analysis 36 (2004) 1159–1162.
[2] M.Z.C. Hu, E.A. Payzant, K.R. Booth, C.J. Rawn, R.D. Hunt, L.F. Allard, Ultrafine microsphere particles of zirconium titanate produced by homogeneous dielectric-tuning coprecipitation, Journal of Materials Science 38 (2003) 3831–3844.
[3] I.C. Cosentino, E.N.S. Muccillo, R. Muccillo, Development of zirconia–titania porous ceramics for humidity sensors, Sensors and Actuators B 96 (2003) 677–683.
[4] J.L. Lakshmi, N.J. Ihasz, J.M. Miller, Synthesis, characterization and ethanol partial oxidation studies of V_2O_5 catalysts supported on TiO_2–SiO_2 and TiO_2–ZrO_2 sol–gel mixed oxides, Journal of Molecular Catalysis A: Chemical 165 (2001) 199–209.
[5] M.E. Zorn, D.T. Tompkins, W.A. Zeltner, M.A. Anderson, Photocatalytic oxidation of acetone vapor on TiO_2/ZrO_2 thin films, Applied Catalysis B 23 (1999) 1–8.
[6] D.V. Shtansky, M.I. Petrzhik, I.A. Bashkova, F.V. Kiryukhantsev-Korneev, A.N. Sheveiko, E.A. Levashov, Adhesion, friction, and deformation characteristics of Ti–(Ca,Zr)–(C,N,O,P) coatings for orthopedic and dental implants, Physics of the Solid State 48 (2006) 1301–1308.
[7] L.Y. Zhu, D. Xu, G. Yu, X.Q. Wang, Preparation and characterization of zirconium titanate fibers with good high temperature performance, Journal of Sol–Gel Science and Technology 49 (2009) 341–346.
[8] J. Macan, A. Gajovi, H. Ivankovic, Porous zirconium titanate ceramics synthesized by sol–gel process, Journal of the European Ceramic Society 29 (2009) 691–696.
[9] L.G. Karakchiev, T.M. Zima, N.Z. Lyakhov, Low-temperature synthesis of zirconium titanate, Inorganic Materials 37 (2001) 386–390.
[10] M. Anarianainarivelo, R.J.P. Corriu, D. Leclercq, P.H. Mutin, A. Vioux, Nonhydrolytic sol–gel process: aluminium and zirconium titanate gels, Journal of Sol–Gel Science and Technology 8 (1997) 89–93.
[11] M. Anarianainarivelo, R.J.P. Corriu, D. Leclercq, P.H. Mutin, A. Vioux, Non-hydrolytic sol–gel process: zirconium titanate gels, Journal of Materials Chemistry 7 (1997) 279–284.
[12] Q.F. Lu, D.R. Chen, X.L. Jiao, Synthesis of long $ZrTiO_4$ fibers by a sol–gel process free of organic components, Journal of Materials Chemistry 13 (2003) 1127–1131.
[13] S.X. Zhang, J.B. Li, J. Cao, H.Z. Zhaim, B. Zhang, Preparation, microstructure and microwave dielectric properties of $Zr_xTi_{1-x}O_4$ ($x=0.40$–0.60) ceramics, Journal of the European Ceramic Society 21 (2001) 2931–2936.
[14] S. Naci Koc, Zirconium titanate synthesis by diethanol amine based sol–gel route, Journal of Sol–Gel Science and Technology 38 (2006) 277–281.
[15] M.C. Barrera, M. Viniegra, J. Escobar, M. Vrinat, J.A. de los Reyes, F. Murrieta, J. García, Highly active MoS_2 on wide-pore ZrO_2–TiO_2 mixed oxides, Catalysis Today 98 (2004) 131–139.
[16] E.L. Sham, M.A.G Aranda, E.M. Farfan-Torres, J.C. Gottifredi, M. Martínez-Lara, S. Bruque, Zirconium titanate from sol–gel synthesis—thermal decomposition and quantitative phase analysis, Journal of Solid State Chemistry 139 (1998) 225–232.
[17] M.R. Mohammadi, D.J. Fray, Synthesis and characterisation of nanosized TiO_2–ZrO_2 binary system prepared by an aqueous sol–gel process: physical and sensing properties, Sensors and Actuators B 155 (2011) 568–576.
[18] H.E. Kissinger, Reaction kinetics in differential thermal analysis, Analytical Chemistry 29 (1957) 1702–1706.
[19] M. Macias, P.J. Sanchez-Soto, J.A. Navio, Kinetic study of crystallization in zirconium titanate from an amorphous reactive prepared precursor, Journal of Non-Crystalline Solids 147–148 (1992) 262–265.
[20] H.R. Wang, Y.L. Gao, G.H. Min, X.D. Hui, Y.F. Ye, Primary crystallization in rapidly solidified $Zr_{70}Cu_{20}Ni_{10}$ alloy from a supercooled liquid region, Physics Letters A 314 (2003) 81–87.
[21] H.P. Klug, L.E. Alexander, X-Ray Diffraction Procedures, J. Wiley, New York, 1974.
[22] J.A. Navio, F.J. Marchena, M. Macias, P.J. Sanchez-Soto, P. Pichat, Formation of zirconium titanate powder from a sol–gel prepared reactive precursor, Journal of Materials Science 27 (1992) 2463–2467.